

Blockade Of Peroxynitrite-Induced Neural Stem Cell Death In The Acutely Injured Spinal Cord By Drug-Releasing Polymer

Dou Yu^{a,b}, William L. Neeley^c, Christopher D. Pritchard^{a,c}, Jonathan R. Slotkin^{a,d}, Eric J. Woodard^d, Robert Langer^{c,e}, Yang D. Teng^{a,b,f*}

^aDepartment of Neurosurgery, Harvard Medical School, the Brigham and Women's Hospital and Children's Hospital Boston, Boston, Massachusetts 02115, USA. ^bDivision of SCI Research, VA Boston Healthcare System, Boston, Massachusetts 02132, USA; ^cDepartment of Chemical Engineering, Massachusetts Institute of Technology, Cambridge, Massachusetts 02139, USA; ^dDivision of Neurological Surgery, New England Baptist Hospital, Boston, Massachusetts 02120, USA; ^eDivision of Health Sciences and Technology, Massachusetts Institute of Technology, Cambridge, Massachusetts 02139, USA; ^fDepartment of Physical Medicine and Rehabilitation, Harvard Medical School, Spaulding Rehabilitation Hospital, Boston, Massachusetts 02114, USA.

Key words. spinal cord injury • neural stem cell • nitric oxide • peroxynitrite • PLGA scaffold, neuroinflammation.

ABSTRACT

Therapeutic impact of neural stem cells (NSCs) for acute spinal cord injury (SCI) has been limited by the rapid loss of donor cells. Neuroinflammation is likely the cause. Since there are close temporal-spatial correlations between the inducible nitric oxide (NO) synthase expression and the donor NSC death after neurotrauma, we reasoned that NO-associated radical species might be the inflammatory effectors which eliminate NSC grafts and kill host neurons. To test this hypothesis, human NSCs (hNSCs: 5×10^4 - 2×10^6 /ml) were treated *in vitro* with "plain" medium, 20 μ M glutamate, or donors of NO and peroxynitrite (ONOO⁻; 100 and 400 μ M of spermine or DETA NONOate, and SIN-1, respectively). hNSC apoptosis primarily resulted from SIN-1 treatment, showing ONOO⁻-triggered protein nitration and the activation of p38 MAPK, cytochrome *c* release, and caspases. Therefore, cell death following post-SCI (p.i.) NO surge may be

mediated through conversion of NO into ONOO⁻. We subsequently examined such causal relationship in a rat model of dual penetrating SCI using a retrievable design of poly-lactic-co-glycolic acid (PLGA) scaffold seeded with hNSCs that was shielded by drug-releasing polymer. Besides confirming the ONOO⁻-induced cell death signaling, we demonstrated that co-transplantation of PLGA film embedded with ONOO⁻ scavenger, manganese (III) tetrakis (4-benzoic acid) porphyrin (MnTBAP) or uric acid (1 μ mol/film), markedly protected hNSCs 24 h p.i. (total: n = 10). Our findings may provide a bioengineering approach for investigating mechanisms underlying the host microenvironment and donor NSC interaction and help formulate strategies for enhancing graft and host cell survival after SCI.

Author contributions: D.Y.: Study design and conduct, collection and/or assembly of data, data analysis and interpretation, manuscript writing; W.L.N.: Study design and conduct, collection and/or assembly of data, data analysis and interpretation, manuscript writing; C.D.P.: Study conduct, collection and/or assembly of data, data analysis and interpretation; J.R.S.: Study design, and data interpretation; E.J.W.: Study design, and data interpretation; R.L.: Conception and study design, academic and financial support, provision of study material, manuscript writing, final approval of manuscript; Y.D.T.: Conception and study design, data analysis and interpretation, financial and administrative support, provision of study material, manuscript writing, final approval of manuscript.

*Corresponding author: Department of Neurosurgery, Harvard Medical School and the Brigham and Women's Hospital, Boston, MA 02115, Email: yang_teng@hms.harvard.edu, (Telephone) 1-617-525-8676, (Fax) 1-617-264-5216. Received August 15, 2008; accepted for publication January 22, 2009; first published online in Stem Cells Express February 5, 2009. ©AlphaMed Press 1066-5099/2009/\$30.00/0 doi: 10.1002/stem.26

INTRODUCTION

Although post-spinal cord injury (SCI; p.i.) neuroinflammation damage persists chronically, the early release of inflammation mediators, reactive nitrogen species (RNS) or reactive oxygen species (ROS) free radicals, may dominate the immediate aftermath of donor cell loss [1, 2]. While the detrimental and beneficial effects of the secondary reactions p.i. are still under debate [3-5], it is largely unknown as to how such neuroinflammatory events affect the survival and therapeutic potential of the undifferentiated neural stem cells (NSCs) *in vivo*. Because of the expression profile difference in surface receptors and intracellular targets between NSCs and mature tissue, the mechanisms underlying adult tissue loss may not be responsible for the acute donor NSC loss post transplantation.

Nitric oxide (NO) and related RNS are a group of radicals linked with the secondary pathology of SCI [1, 4, 5]. There are close temporal correlations between the enhanced inducible nitric oxide synthase (iNOS) expression after injury and the death of NSC grafts [6-8] (i.e., within the first 12-72 h after injury), indicating a possible role for RNS radicals in triggering the cell graft loss. Additionally, NSCs do not express ionotropic glutamate receptors as mature neurons do, circumventing the NMDA-receptor mediated Ca^{2+} influx, or anoxia induced sodium influx [9-11]. Massive activation of iNOS increases tumor suppressor protein p53, cytochrome *c* release, chromatin condensation, and DNA fragmentation [12, 13], causing apoptosis of the target cells [14]. Bursts of NO and superoxide (O_2^-) are produced by activated inflammatory cells, and these radicals combine in a diffusion-limited reaction to form the highly reactive peroxynitrite (ONOO^-). ONOO^- quickly combines with CO_2 to form nitroperoxycarbonate, which rapidly decomposes to form carbonate radical and nitrogen dioxide, two potentially reactive radicals that are believed to be responsible for the

deleterious cellular effects of ONOO^- [15]. Recent *in vitro* studies using a donor of NO or ONOO^- demonstrated that these molecules could induce apoptosis in murine NSCs or primary neurons through p38 MAP kinase (MAPK) signaling, and p21-MAPK-p19 induced p53 accumulation [16, 17]. Correspondingly, activation of caspases and apoptosis in neurons could be blocked by p38 MAPK inhibitors [18]. Conversely, the roles of NO in neurogenesis and stem cell differentiation have also been explored extensively [19], including the neuroprotective roles of appropriate doses of NO in some neurodegenerative diseases [20, 21]. These results raise the possibility that NO is an upstream signaling molecule that can turn on protective or destructive pathways depending on its dose and derivatives as well as the target cell's developmental or pathophysiological status. Therefore, we hypothesized that insults by inflammation mediators such as RNS and ROS radicals may be largely responsible for the death of donor human NSCs (hNSCs) implanted acutely following SCI. Since NSCs produce neurotrophic factors, induce host tissue regeneration, facilitate rebuilding of the synaptic network, and activate compensatory mechanisms dormant during physiological conditions [22-25], impeding the causal factors of donor loss may augment the timely presence of NSCs at the injury epicenter p.i., which is crucial towards the restoration of tissue homeostasis to invoke neuroplasticity [26, 27]. We have now tested the roles of NO and ONOO^- on the survival of hNSCs *in vitro* as well as in the p.i. spinal cord by establishing a novel approach of identifying cell death signals via interactive systems of hNSCs and compound-embedded polymers, and using scavenger-releasing poly-lactic-co-glycolic acid (PLGA) polymer films to protect hNSCs *in vivo* p.i. [28].

MATERIALS AND METHODS

All chemicals were purchased from Axxora (San Diego, CA) unless specified otherwise. (Z)-1-{N-[3-Aminopropyl]-N-[4-(3-aminopropylammonio)butyl]-amino}-diazene-1-ium-1,2-diolate (Spermine NONOate) and (Z)-1-[2-(2-Aminoethyl)-N-(2-ammonioethyl)amino]diazene-1-ium-1,2-diolate (DETA NONOate), were used as NO donors in the medium. For detailed information regarding items listed below, see Supplementary Information.

Culture and pharmacological treatments of hNSCs Human fetal brain neural progenitor cells [29] (polyclonal cell line HFB2050) were maintained in serum free NeurobasalTM medium (Invitrogen, Grand Island, NY) containing a combination of growth factors at 37°C in a humidified 5% CO₂/air incubator.

Cell death assays Apoptosis assays were run with reagent kits (Roche Applied Sciences, Indianapolis, IN). Caspase assays were run with the ApoAlertTM Caspase Fluorescent Assay Kits (BD Biosciences, San Diego, CA). Immunoblotting and immunocytochemistry (ICC) for cytochrome *c* and upstream signals were performed as previously described [12, 13, 30].

Fabrication of scavenger-releasing PLGA films and drug release capacity assessment To assess the effects of ONOO⁻ qualitatively *in vivo*, we prepared PLGA-scavenger depots using appropriate organic solvents [31]. In a 1:10 weight ratio design, uric acid (UA: 3.4 mg; ~20 μmol) was suspended in a solution of PLGA (34 mg) dissolved in 800 μl CH₂Cl₂, and manganese (III) tetrakis (4-benzoic acid) porphyrin (MnTBAP: 10 mg; ~11 μmol) dissolved in 454 μl tetrahydrofuran containing 100 mg PLGA. Subsequently, a drop of the mixture (20 μl) was disposed onto a coverglass and allowed to form a uniformly thin film. This results in each coverglass carrying 0.5 μmol scavenger per film after the organic solvent evaporation.

Additionally, a 1:3 weight ratio between MnTBAP and PLGA was used to produce 1 μmol scavenger films.

We measured the drug release time-course by UV spectroscopy. Briefly, scavenger-embedded PLGA films were incubated in medium with either 0, 0.5, or 1.0 million cells per unit. Samples were taken from each unit at 5, 24, 48, 72, and 168 h, immediately frozen, and stored at -20 °C. To determine the total amount of MnTBAP released, 100 μl of each sample were mixed with 100 μl of 600 mM potassium phosphate buffer at pH 7.0. For UA, 20 μl of each sample were mixed with 100 μl of the potassium phosphate buffer and 80 μl of deionized water. The absorbance of MnTBAP at λ = 468 nm and of UA at λ = 293 nm were read using the extinction coefficients of 93000 M⁻¹ cm⁻¹ for MnTBAP [32] and 12000 M⁻¹ cm⁻¹ for UA [33] to calculate the released amount of each drug.

To evaluate whether the drug embedded in PLGA films still retained ONOO⁻-scavenging capability, we used the selective fluorescent indicator for ONOO⁻, dihydrorhodamine 123 (DHR123), to measure the levels of ONOO⁻ in the medium after the ONOO⁻ donor, SIN-1 chloride (3-morpholinonydnonimine [product number: ALX-430-002]; SIN-1) was co-incubated with PLGA films embedded with MnTBAP. Each cell medium was sampled in 30 min intervals with a 200 μl unit volume, and the level of ONOO⁻ was measured at λ_{ex} = 500 nm and λ_{em} = 536 nm after DHR123 was dissolved (final dilution: 10 μM).

Assessment of the neuroprotective effects of drugs embedded in PLGA polymers *in vivo*

Adult female Sprague-Dawley rats (225 - 250 g; total: n = 10; Charles River Labs, Wilmington, MA) were used for the creation of two penetrating injuries per rat at T7-T8 and L2-L3, respectively (Fig. 1). All animal protocols were in accordance with the Harvard Medical School IACUC guidelines. For each SCI site, midline hemisections were created using a size 11 scalpel

[24], under adequate anesthesia [30]. Spinal cord tissue between the hemisections was removed using a pair of iris scissors (injury gap length: 2 mm; [24]), and hemostasis was achieved using Gelfoam™ (Pfizer, New York, NY). For the non-retrieval study evaluating the implant effect on host tissue (total: n = 6), a circular PLGA polymer film ($\phi = 4$ mm; thickness: ~ 500 μm) embedded with MnTBAP or UA (n = 3 for each) was inserted into either T7-T8 or L2-L3 epicenter to cover the ventral bottom first, and wrap up the lateral side of the implanted porous PLGA scaffold (300 - 400 μm pore size; dimensions: 2 x 3 x 2, unit: mm) seeded with hNSCs. Inside the other injury epicenter, a PLGA polymer film not embedded with drug was used as a control treatment. Thus, with the two SCI sites (T7-8 vs. L2-3) well separated, and the second injury being done immediately following the first one as well as the two loci alternated for receiving the treatments in different animals, our dual penetrating SCI model eliminates common variables incurring in cross-animal studies, and renders other elements potentially affecting donor cell survival (e.g., blood circulation, edema, etc.) as systematical factors for either SCI site (see Results for comparable outcomes). Twenty four h p.i., the re-anesthetized rats were perfused for histopathological analysis, as previously reported [24].

Systematical and unbiased cell counting In a separate experiment series (n = 4), scaffolds seeded with hNSCs were wrapped in a nylon-net shell with 30 μm pore size (Millipore, Billerica, MA) prior to implantation, and PLGA films embedded with MnTBAP (drug protection) and plain PLGA films (control) were used in combination to study the effects of drug protection on donor hNSC survival (Fig. 1). The animals were re-anesthetized 24 h p.i., and the scaffolds wrapped in nylon net removed prior to perfusion of the animals. The removed scaffolds were immediately immersed in 4% paraformaldehyde (PFA) in 0.1M PB for overnight fixation, cryoprotected in 30% sucrose, separated from the nylon net shell using

a size 15 scalpel, embedded in OCT compound, and cut into 20 μm serial sections for ICC analysis. Our cell quantification methods were adapted from previous studies [34]. Briefly, the retrieved scaffolds with comparable dimensions ($2\pm 0.1 \times 2.5\pm 0.3 \times 1.8\pm 0.2$, unit: mm; n = 4 [dual injuries] for scaffolds with MnTBAP protection, or without drug protection, respectively) were embedded in pairs with the same orientation. Serial 20 μm sections were cryostatted, and 8 sections 200 μm apart from each other sequentially sampled from each series. Pre-implantation hNSC-seeded scaffolds (n = 6) were used as intact controls. Sections were then double-labeled for ICC identification of hNSCs (hNestin [1:200; Millipore, Billerica MA] coupled with DAPI nuclei staining [Vector Labs, Burlingame, CA]), and hNSCs underwent apoptosis (using antibodies against cleaved caspase 3 [1:100; Cell Signaling, Danvers, MA]). The use of 50 μm grids for quantifying cells in a single section together with sampling the adjacent sections 200 μm apart ensured that no estimate inflation occurred due to repeated counting of the same cells. The total number of hNSCs (i.e., hNestin positive cells) in each section was recorded for deriving the percentage of apoptotic hNSCs (i.e., presenting cleaved caspase 3).

RESULTS

ONOO⁻, but not NO, induces hNSC apoptosis

The following series of cell death assays were run to compare the effects of NO and ONOO⁻ on hNSCs using specific donors of either molecules: spermine NONOate for NO, and SIN-1 for ONOO⁻, which have similar half-lives in solution, (39 min and 26 min at 37°C, respectively). The oxygen consumption due to the breakdown of SIN-1 was monitored, and a 10-15% O₂ level drop was observed using a dissolved oxygen (DO) meter (Jenco) 90 min after the donors were added to the solution (Supplementary Figure 1). To avoid the potential pro-apoptotic impacts resulting from low levels of DO in the cell culture medium, we replenished the culture solution with fresh

medium containing freshly dissolved SIN-1 every 30 min during the 3 h of incubation.

Outcomes of annexin V-FLUOS assay In Fig. 2a-e, all the tri-channel images of the hNSCs attached to coverglass showed no intracellular presence of propidium iodide (PI: red), indicating that necrosis due to compromised membrane integrity and intracellular diffusion of PI did not yet occur after the 3 h drug stimulation. Green fluorescence with a clear cellular outline profile, conversely, is specifically indicative of apoptosis when annexin V binds to the translocated phosphatidylserine on the external cell surface. Under control conditions, some green fluorescence could be observed, but appeared to be trapped mainly in spaces between cells resulting, perhaps, from insufficient washing (Fig. 2a). In contrast, stimulation with 400 μM SIN-1 led to strong green fluorescence on the outer surface of hNSCs, showing a clear cell body profile (Fig. 2b). Co-incubation with scavenger for ONOO⁻, MnTBAP (100 μM) or UA (100 μM), eliminated the effect (Fig. 2c, d). To detect the possible roles of excitotoxicity in causing the acute death of hNSC post implantation, we used glutamate stimulation (20 μM for 3 h; normal CSF glutamate level is ~ 0.3 μM [35]) to trigger excitotoxicity in hNSCs; neither apoptotic nor necrotic cell death was observed (Fig. 2e). Similar outcomes were seen in hNSCs suspensions (Fig. 2f). Lastly, cell counting indicated that spermine NONOate did not induce similar levels of cell death as SIN-1 exposure did in a dose dependent manner.

TUNEL assay results To further verify the findings of annexin V-FLUOS assay, we incubated hNSCs with reagents of the TUNEL assay kit for 1 h at 37°C after hNSCs were fixed in 4% PFA and permeabilized following stimulation using NO and ONOO⁻ donors. TUNEL was designed for labeling DNA strand breaks that occur during the early stages of apoptosis; in controls, virtually no green fluorescence was seen in either the attached hNSCs (Fig. 3a) or hNSCs in suspension (Fig.

3e). NO donor spermine NONOate did not cause apoptosis in these cells (Fig. 3e), consistent with the result of annexin V-FLUOS assay. By contrast, SIN-1 treatment dose-dependently induced DNA breakage in hNSCs in both the attached (Fig. 3b) and suspension forms (Fig. 3e), mimicking the effects of DNase I (i.e., the positive controls; Fig. 3e) and in agreement with annexin V-FLUOS assay results. The addition of the ONOO⁻ scavengers MnTBAP (100 μM) or UA (100 μM) blocked the apoptotic effect of SIN-1 and rendered the outcomes similar to those of the controls, providing further evidence that ONOO⁻ causes hNSC apoptosis, but not NO.

Nitrotyrosine footprinting in hNSCs ONOO⁻ reacts with target proteins and leaves behind the end product nitrotyrosine, a reliable marker for the functional presence of ONOO⁻ [20]. Using ICC staining for nitrotyrosine, we confirmed that the deleterious effects of SIN-1 were indeed due to the elevated levels of ONOO⁻ nitration (Fig 4), which was completely absent in controls and efficiently prevented by co-incubation with ONOO⁻ scavengers MnTBAP or UA (Fig. 4).

In summary, the aforementioned *in vitro* experiments clearly demonstrate that ONOO⁻ exposure results in hNSC death, and treatments that scavenge ONOO⁻ can prevent the lethal effects of ONOO⁻ on hNSCs.

Identification of the signaling pathways involved in the effects of NO or ONOO⁻ on hNSCs

The outcome measurements listed below demonstrate the molecular pathways underlying the effects of NO or ONOO⁻ on hNSCs. ONOO⁻ has been linked with several cell death signaling pathways in genetically engineered murine cells manifesting NSC-like properties [16], or other cell types [36], among which the activation of p38 MAPK, and cytochrome *c* release from mitochondria were shown to underlie the pro-apoptotic effects of ONOO⁻ and the eventual activation of caspases. Though we speculated that multiple signaling pathways likely co-exist in the *in vivo* settings, we believed that clear

targets along each specific signaling pathway should be identified, so that anti-apoptosis strategies might be developed to enhance the post-implantation survival of hNSCs in addition to identifying hNSC-related cell death signaling pathways. For the present study, we focused on one of the well reported signaling pathways: ONOO⁻ - p38 MAPK - cytochrome *c* release - caspase activation.

Western Blot and ICC analysis of upstream signaling pathways

Erk (a signaling kinase of cell survival which can be activated by free radicals; [16, 17]) and p38 MAPK phosphorylation were examined by Western Blot. Using total Erk or total p38 MAPK as control proteins to ensure equal sample loading, we probed for their phosphorylated forms. Both Erk and p38 MAPK were shown strongly phosphorylated in cells treated with SIN-1 (400 μ M) alone (Fig. 5a, b), but not with spermine NONOate (400 μ M). Treatment with MnTBAP (200 μ M) or UA (200 μ M) attenuated the SIN-1 effect. The phosphorylation of p38 MAPK could be localized to mitochondria, as shown in the double-labeling ICC using antibodies against both phospho-p38 MAPK (arrows, Fig. 5c, red) and human mitochondria (hMito; Fig. 5c, green dots). The phosphorylation of p38 MAPK could be correlated to the translocation of cytochrome *c* from the mitochondria to the cytosol in hNSCs stimulated with SIN-1 (400 μ M), which was shown in Western Blots using separated protein samples from either the mitochondria or cytosol fractions of the cell homogenate (Fig. 5d). COX4 and beta-actin were used as control proteins for the mitochondria and cytosol fractions, respectively, to ensure that an equal amount of total proteins were sampled. After 6 h of stimulation, SIN-1 exposure dose dependently (100, 400 μ M) induced the mitochondrial release of cytochrome *c* to the cytosol, mimicking the effect of the positive control, staurosporine stimulation (0.2 μ g/ml). DETA NONOate (100, 400 μ M), however, did not have the same effect. Diffuse labeling of cytoplasmic cytochrome *c* (arrows, green, Fig. 5e) could be seen only in

cells stimulated by SIN-1 for 3 h, but not in controls. Co-incubation with MnTBAP (100 μ M) or UA (100 μ M) blocked the translocation. Finally, both Western Blot and ICC demonstrated that incubation with SIN-1 also increased the activation of caspase 3, but not when co-incubated with MnTBAP or UA (Fig. 5f, g). Our data indicated that SIN-1 stimulation initiated a cascade of apoptotic events inside the hNSCs, which led to hNSC apoptosis as detected in the apoptosis assays. Moreover, the activation of each key signaling molecule could be blocked or markedly attenuated by ONOO⁻ scavenging.

Fluorescent detection of the activation of Caspase 3, 8, and 9 Fluorescence-labeled substrates for caspase 3, 8, and 9 were used to exhibit the activation of these caspases quantitatively based on the color shift. Fig. 5h shows the detected fluorescent levels of each enzymatic reaction in the hNSCs treated with spermine NONOate or SIN-1, with or without MnTBAP. These data indicate that caspase 9 and its downstream effector caspase 3 were activated by ONOO⁻, but not by NO; however, the effects of ONOO⁻ could be eliminated by MnTBAP, an outcome that was consistent with the findings of other assays showing that NO itself did not induce hNSC apoptosis. Our results also suggested that caspase 8 was not involved in the apparent pro-apoptotic effects of ONOO⁻ on the hNSCs *in vitro* (data not shown).

Drug-releasing PLGA films and their capability to scavenge ONOO⁻

We then proceeded to embed MnTBAP or UA in PLGA films, so that we could ultimately implant hNSC-seeded scaffolds together with drug-releasing PLGA films to test the ability of these drugs to inhibit the effects of ONOO⁻ on hNSCs *in vivo*. We embedded ONOO⁻ scavengers in the PLGA films to ensure localized and continuous supply of the scavengers to the intended target: the implanted hNSCs and the host tissue at the injury epicenter p.i. A schematic demonstration of how the *in vivo* experiments were conducted is presented in Fig. 1. In our design, the implementation of the porous nylon net was

intended to ensure a clean removal of the scaffolds 24 h post implantation, without interfering with the exposure of donor hNSCs to the endogenous RNS radicals. This initial step toward the definitive *in vivo* SCI study was taken to confirm that drugs were indeed embedded in the polymer films and they could be released to impact the adjacent microenvironment over time.

Because of the difficulties with accurately measuring the total volume of tissue fluid exposed to the drug-releasing PLGA film and the rate of PLGA polymer degradation at the injury epicenter *in vivo*, using a parallel *in vitro* system to characterize the drug-releasing capabilities became a reasonable alternative for proof of principle. In this setting, plain cell culture medium or medium with measurable cell numbers and fluid volume could be used to estimate drug-releasing profiles quantitatively, thus enabling us to assess the basic releasing dynamics of the drug-embedded PLGA films.

To do so, we first measured the release of embedded drugs from the films in plain cell culture medium. Our data showed a sustainable release of MnTBAP and UA embedded, respectively, in the PLGA films (Fig. 6a). Interestingly, the presence of hNSCs in the cell medium expedited the release (Fig. 6b). However, UA demonstrated a faster rate of release than MnTBAP, probably due to its smaller molecular size and higher aqueous solubility, which led to less restraint by the PLGA polymer.

The efficacy of the drug released from the polymer film to scavenge ONOO⁻ was another concern since it was not immediately clear whether the fabrication process of the drug-releasing polymer films altered the reactivity of these drugs. Therefore, we used DHR 123, a specific fluorescent indicator for ONOO⁻, to quantify the levels of ONOO⁻ in cell culture medium containing the same doses of SIN-1 (400 μM), with or without the MnTBAP-releasing films [37]. The results indicate that PLGA films embedded with MnTBAP (1

μmol/film) adequately scavenged ONOO⁻ (Fig. 6c). Hence, modifying the drug: polymer composition weight ratio in the films could change the dynamics of drug release as well as the resultant scavenging capability in the culture medium. We then used such drug-release dynamics obtained *in vitro* to guide the implant design for the following *in vivo* studies.

***In vivo* experiments using drug-releasing PLGA films to protect donor hNSCs**

The roles of ONOO⁻ in the acute donor hNSC death p.i. *in vivo* was verified by eliminating implantation site ONOO⁻ with co-implanted scavenger-releasing PLGA films. Based on the *in vitro* scavenger-releasing dynamics (Fig. 6), we co-implanted hNSC-seeded scaffold with PLGA films embedded with MnTBAP or UA (1 μmol/film) in one hemisection site, and with "plain" films in the other (Fig. 1). At 24 h p.i., analysis of the retrieved scaffolds showed phosphorylation of p38 MAPK in hNSCs that were co-transplanted with control polymer films (Fig. 7a-, arrows), whereas with the protection from PLGA films embedded with an ONOO⁻ scavenger, most hNSCs at the injury epicenter did not have elevated p38 phosphorylation (Fig. 7a+). Accordingly, the levels of nitrotyrosine in the hNSCs were high and present in almost every hNSCs that were co-transplanted with plain polymer film (Fig. 7b-, arrows); however, PLGA films embedded with an ONOO⁻ scavenger prevented nitrotyrosine accumulation in most hNSCs. ICC on caspase 3 activation revealed that without ONOO⁻ scavenger protection, the majority of donor hNSCs underwent acute apoptosis mediated via caspase 3 activation (Fig. 7c-). By contrast, ONOO⁻ scavengers released from the PLGA films provided effective protection against apoptosis of hNSCs during the acute stage p.i. (Fig. 7c+). ICC-based morphological analysis of the epicenter tissue of the injured spinal cord also showed that scaffolds seeded with hNSCs under the scavenger protection were more effective in preventing secondary cellular damage 24 h p.i. For instance, without the presence of PLGA films containing ONOO⁻ scavenger, levels of

both the active caspase 3 and nitrotyrosine were higher in the host tissue 24 h p.i. (Fig. 7d-), relative to those with protection from scavengers embedded in PLGA films (Fig. 7d+). These facts suggested that MnTBAP released from local polymers scavenged ONOO⁻; CSF circulation, which is compromised following penetrating SCI, did not carry any effective drug doses to the control site. Outcomes of the cell counting study further confirmed conclusions drawn from ICC analyses (Fig. 7). Using an unbiased cell quantification method [see Methods], we calculated the percentage of apoptotic hNSCs (i.e., presenting cleaved caspase 3) among total hNSCs (i.e., hNestin-positive cells) in sections sequentially sampled from each polymer implant that was retrieved from the SCI epicenter at 24 h p.i. (n = 4 for scaffolds with MnTBAP protection, or without drug protection, respectively). Pre-implantation hNSC-seeded scaffolds (n = 6) were used as intact controls. We found that relative to the control implants, MnTBAP-releasing film significantly reduced the average percentage of hNSCs carrying activated caspase 3, with mitigation rates ranging from ~40 to ~70% at different loci systematically sampled along the entire length of the implant (p < 0.005 - 0.0004, paired *t*-test; supplementary Fig. 2c). Interestingly, scaffolds with MnTBAP also yielded significantly higher total hNSC numbers after retrieval, compared with the controls (supplementary Fig. 2a). Taken together, these *in vivo* experimental data, analyzed *in situ* or *in vitro*, suggest that ONOO⁻ indeed plays a major role in donor hNSCs death in the acutely injured spinal cord.

DISCUSSION

Functional deficits resulting from traumatic SCI are due to the loss of mature axons and neurons. In addition, the extracellular microenvironment that supports proper inter-neuronal activity is also severely damaged, with consequent inflammatory events rendering the injury site uninhabitable to donor stem cells [1]. Therefore, the effective regeneration of the spinal cord requires two main elements: donor cells with

remarkable regenerative capabilities and a pro-regenerative extracellular microenvironment that promotes donor cell survival and proper differentiation, the re-growth of host axons, and the functional reorganization of the neurites and neural circuitries (i.e., neural plasticity).

To date, effective therapy for SCI using stem cells is still far from reality. One of the most challenging barriers may reside in an important aspect of the p.i. pathology: the swift development of toxicity and inflammation at the injury epicenter that can jeopardize the initial survival and repair potential of the donor cells [38]. Post-injury pathophysiology usually involves two processes: the primary injury, mostly caused by mechanical insults, and the secondary injury events (within minutes to weeks or even months after SCI), in which heightened release of pro-inflammatory cytokines (e.g., TNF- α and IL-1 β) [39-41]; oxidative stress, ischemia, and free radicals produced by leukocytes, macrophages and microglia; glutamate metabolism impairment due to cytokines and free radicals leading to excitatory cytotoxicity [42, 43]; breakdown of the blood-brain barrier and neural tissues by phospholipase A2, arachidonic acid, eicosanoids, extracellular matrix-degrading enzymes such as metalloproteinase [1, 44-48]; pathological autoimmune response mediated by activated lymphocytes; all leading to protein nitration, breaking down of lipids and nucleic acids, demyelination and apoptosis as well as neuroinflammation. This complex cascade of interactive events not only exacerbates tissue/cell loss, but also impedes repair mechanisms through, for instance, limiting the survival of the donor cells [49]. In fact, observations made by others and our own group indicate that only a very small amount of the donor cells (i.e., \leq 1-2%) could survive beyond the initial 7-10 days if implanted immediately following SCI; conversely, delayed transplantation showed improved grafting in the lesioned spinal cord [50]. Hence, there is an evident need to develop *in vivo* strategies to overcome the early stage donor cell loss following SCI. Though there are

multiple cell death pathways activated by SCI, by limiting the study window to 24 h p.i., we were able to identify that ROS and RNS radicals present at the epicenter, such as those produced by ONOO⁻, appear to play critical roles in triggering cell death, and, in a broader sense, mediating inflammation after SCI. Importantly, effective measures to slow down these changes provided by drug-releasing scaffolds mitigated the activation of cell death signals and significantly augmented hNSC survival. Donor cell survival beyond 24 h is certainly a critical goal for therapeutic development. Though 24-h p.i. offers an effective window for examining the roles of ONOO⁻ [1, 7], we are currently investigating longer term protective impacts of our approach [51], which will be published separately in the future.

The development of oxidative stress following SCI involves ROS and RNS toxicology [52, 53]. In contrast to other common secondary inflammatory or neurotoxic signals, NO benefits stem cell development at basal physiological levels but becomes detrimental when its concentration spikes, such as during the inflammatory response [5, 54, 55]. Our results showed that the surge in ONOO⁻ is an integral and essential component of the secondary injury event that compromises donor hNSC survival and exacerbates tissue damages p.i. Although there are natural defense mechanisms in the CNS against the variety of oxidants, namely ascorbic acid (vitamin C, a hydrophilic antioxidant), α -tocopherol (vitamin E, a hydrophobic antioxidant, against lipid peroxidation), glutathione (an intracellular tripeptide, scavenges ROS radicals), lipoic acid, uric acid, and enzymes such as superoxide dismutase (SOD), catalase, and glutathione peroxidase (degrading O₂⁻ and hydroxyl radical [·OH]). Neurotrophic factors autocrined or supplied to NSCs also facilitate their survival against oxidative insults [56, 57]. The activation of Erk signaling pathways, often associated with cell protection and survival mechanisms, is a confirmation that hNSCs possess innate defense mechanisms. However, these endogenous barriers do not

appear sufficient to prevent donor loss during the acute phase of SCI. In our studies, we used membrane-permeable MnTBAP, a compound belonging to the family of metalloporphyrins that scavenge O₂⁻ through the dismutation reaction and possess peroxidase activity (protecting cells from H₂O₂), to remove ONOO⁻ and inhibit lipid peroxidation [37, 58, 59]. MnTBAP was previously shown to counteract the deleterious effects of RNS and ROS free radicals in multiple neurological disease models [60-63]. Encouragingly, a recent report indicates that relative to other cell types, NSCs have active anti-oxidation mechanisms and seem to recover faster from the initial oxidative stress insults via up-regulation of the antioxidant enzymes through, for instance, uncoupling protein 2 and glutathione peroxidase [56]. Our experiments using high dose glutamate (20 μ M) treatment *in vitro* dismissed any direct cytotoxic effect of glutamate on the cultured hNSCs during the 3 h incubation period (Fig. 2e, f), indicating that the hNSCs routinely used in our studies are too premature to express glutamate receptors to mediate excitotoxicity [29, 64]. Nevertheless, the reported link between glutamate-mediated neurotoxicity and ROS/RNS radicals via NMDA receptor-mediated arachidonic acid release or NOS activation warrants further investigation for its potential role in tissue damage after SCI [65-68]. Additional study regarding the endogenous defense mechanisms in NSCs at both physiological and inflammatory states would help to devise strategies of enhancing the innate survival mechanisms.

The present *in vitro* study outcomes suggest that unlike the extensive cell signaling roles of S-nitrosylation by NO that stabilize factors like HIF-1 α to enhance post-hypoxia/injury repair [69-71], ONOO⁻ likely activates the p38 MAPK-cytochrome *c* release-caspase activation signaling pathways, triggering a key signal that induces hNSC death. Although additional signaling pathways may be involved in the *in vitro* and *in vivo* conditions downstream to ONOO⁻ to cause hNSC death, our conclusion is further supported by the *in vivo* data, confirming

the pro-apoptotic roles of ONOO⁻ and the cytoprotection provided by scavenging it. Therefore, reagents against specific signaling molecules along the cell death pathways induced by ONOO⁻, such as P38 MAPK and caspases, in theory, can potentially be co-implanted for additional protection.

In summary, by pharmacologically targeting RNS radicals, one of the most important groups of signaling molecules for initiating secondary injury processes, via tactics of chemical engineering and stem cell biology, our multimodal studies have provided the first measurable approach to identify molecularly the cause of poor hNSCs survival post implantation *in vivo* after SCI. Using the findings of this experiment as a launching pad, we plan to verify the involvement of pro-inflammation cytokines, glutamate, and other toxic elements further in the *in vivo* environment, so that effective development of therapeutic strategies targeting major secondary pathology following SCI can be facilitated.

ACKNOWLEDGMENTS

Support was received from NIH NS053935, the VA biomedical laboratory research grant and Massachusetts SCI cure research grant (Teng Lab); and NIH Ruth L. Kirschstein National Research Service Award 1F32EY018285-01 for W.L.N., NIH DE013023 and HL060435 (Langer Lab). The authors thank InVivo Therapeutics for the support to their labs. We are grateful to Dr. Martin Feelisch and Dr. William D. Eldred of Boston University for advice on the biochemistry and biology of nitric oxide, and Dr. Robert M. Friedlander of Harvard Medical School for help in studying cell death pathways. We greatly appreciate the grant support from New England Baptist Hospital (Teng Lab).

The authors indicate no potential conflicts of interest.

REFERENCES

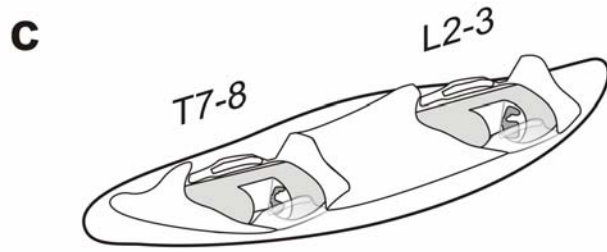
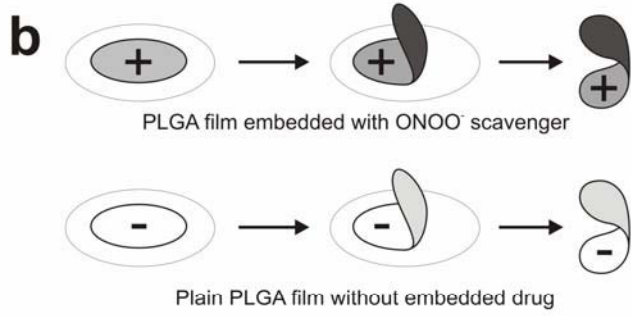
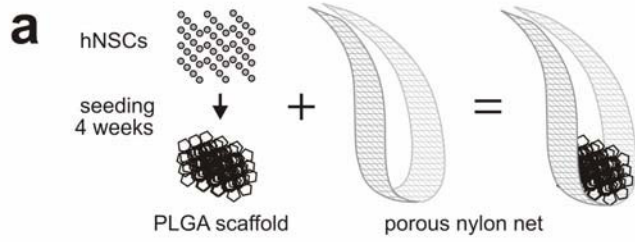
1. Donnelly DJ, Popovich PG. Inflammation and its role in neuroprotection, axonal regeneration and functional recovery after spinal cord injury. *Exp Neurol* 2008;209:378-388.
2. Bramlett HM, Dietrich WD. Progressive damage after brain and spinal cord injury: pathomechanisms and treatment strategies. *Prog Brain Res* 2007;161:125-141.
3. Crutcher KA, Gendelman HE, Kipnis J et al. Debate: "is increasing neuroinflammation beneficial for neural repair?". *J Neuroimmune Pharmacol* 2006;1:195-211.
4. Zhou L, Wu W. Antisense oligos to neuronal nitric oxide synthase aggravate motoneuron death induced by spinal root avulsion in adult rat. *Exp Neurol* 2006;197:84-92.
5. Xu M, Ng YK, Leong SK. 2000. Neuroprotective and neurodestructive functions of nitric oxide after spinal cord hemisection. *Exp Neurol* 2000;161:472-480.
6. Nakahara S, Yone K, Setoguchi T et al. Changes in nitric oxide and expression of nitric oxide synthase in spinal cord after acute traumatic injury in rats. *J Neurotrauma* 2002;19:1467-1474.
7. Chatzipanteli K, Garcia R, Marcillo AE et al. Temporal and segmental distribution of constitutive and inducible nitric oxide synthases after traumatic spinal cord injury: effect of aminoguanidine treatment. *J Neurotrauma* 2002;19:639-651.
8. Díaz-Ruiz A, Ibarra A, Pérez-Severiano F et al. Constitutive and inducible nitric oxide synthase activities after spinal cord contusion in rats. *Neurosci Lett* 2002;319:129-132.
9. Lladó J, Haenggeli C, Maragakis NJ et al. Neural stem cells protect against glutamate-induced excitotoxicity and promote survival of injured motor neurons through the secretion of neurotrophic factors. *Mol Cell Neurosci* 2004;27:322-331.
10. Hsieh WY, Hsieh YL, Liu DD et al. Neural progenitor cells resist excitatory amino acid-induced neurotoxicity. *J Neurosci Res* 2003;71:272-278.
11. Teng YD, Wrathall JR. Local blockade of sodium channels by tetrodotoxin ameliorates tissue loss and long-term functional deficits resulting from experimental spinal cord injury. *J Neurosci* 1997;17:4359-4366.
12. Radi R, Cassina A, Hodara R. Nitric oxide and peroxynitrite interactions with mitochondria. *Biol Chem* 2002;383:401-409.
13. Brunori M, Giuffrè A, Forte E et al. Control of cytochrome c oxidase activity by nitric oxide. *Biochim Biophys Acta* 2004;1655:365-371.

14. Brüne B, von Knethen A, Sandau KB. Nitric oxide and its role in apoptosis. *Eur J Pharmacol* 1998;351:261-272.
15. Dedon PC, Tannenbaum SR. Reactive nitrogen species in the chemical biology of inflammation. *Arch Biochem Biophys* 2004;423:12-22.
16. Cheng A, Chan SL, Milhavet O et al. p38 MAP kinase mediates nitric oxide-induced apoptosis of neural progenitor cells. *J Biol Chem* 2001;276:43320-43327.
17. Kaji T, Kaieda I, Hisatsune T et al. 3-Morpholinopyridone hydrochloride induces p53-dependent apoptosis in murine primary neural cells: a critical role for p21(ras)-MAPK-p19(ARF) pathway. *Nitric Oxide* 2002;6:125-134.
18. Ghatan S, Larner S, Kinoshita Y et al. p38 MAP kinase mediates bax translocation in nitric oxide-induced apoptosis in neurons. *J Cell Biol* 2000;150:335-347.
19. Gibbs SM. Regulation of neuronal proliferation and differentiation by nitric oxide. *Mol Neurobiol* 2003;27:107-120.
20. Keynes RG, Garthwaite J. Nitric oxide and its role in ischaemic brain injury. *Curr Mol Med* 2004;4:179-191.
21. Deckel AW. Nitric oxide and nitric oxide synthase in Huntington's disease. *J Neurosci Res* 2001; 64:99-107.
22. Thuret S, Moon LD, Gage FH. Therapeutic interventions after spinal cord injury. *Nat Rev Neurosci* 2006;7:628-643.
23. Goldman SA, Windrem MS. Cell replacement therapy in neurological disease. *Philos Trans R Soc Lond B Biol Sci* 2006;361:1463-1475.
24. Teng YD, Lavik EB, Qu X et al. Functional recovery following traumatic spinal cord injury mediated by a unique polymer scaffold seeded with neural stem cells. *Proc Natl Acad Sci U S A* 2002;99:3024-3029.
25. Murray M, Fischer I. Transplantation and gene therapy: combined approaches for repair of spinal cord injury. *Neuroscientist* 2001;7:28-41.
26. Raisman G, Li Y. Repair of neural pathways by olfactory ensheathing cells. *Nat Rev Neurosci* 2007;8:312-319.
27. Teng YD, Liao WL, Choi H et al. Physical activity-mediated functional recovery after spinal cord injury: potential roles of neural stem cells. *Regen Med* 2006;1:763-776.
28. Karp JM, Langer R. Development and therapeutic applications of advanced biomaterials. *Curr Opin Biotechnol* 2007;18:454-459.
29. Redmond DE Jr., Bjugstad KB, Teng YD et al. Behavioral improvement in a primate Parkinson's model is associated with multiple homeostatic effects of human neural stem cells. *Proc Natl Acad Sci U S A* 2007;104:12175-12180.
30. Teng YD, Choi H, Onario RC et al. Minocycline inhibits contusion-triggered mitochondrial cytochrome c release and mitigates functional deficits after spinal cord injury. *Proc Natl Acad Sci U S A* 2004;101:3071-3076.
31. Grayson AC, Cima MJ, Langer R. Size and temperature effects on poly(lactic-co-glycolic acid) degradation and microreservoir device performance. *Biomaterials* 2005;26:2137-2145.
32. Harriman A, Porter G. Photochemistry of manganese porphyrins. *J Chem Soc* 1979;Faraday Trans 275:1532-1542.
33. Kalckar HM. Differential spectrophotometry of punne compounds by means of specific enzymes. I. Determination of hydroxypurine compounds. *J Biol Chem* 1947;167:429-443.
34. Teng YD, Mocchetti I, Wrathall JR. Basic and acidic fibroblast growth factors protect spinal motor neurones in vivo after experimental spinal cord injury. *Eur J Neurosci* 1998;10:798-802.
35. Fonnum F. Glutamate: a neurotransmitter in mammalian brain. *J Neurochem* 1984;42:1-11.
36. Zhang Y, Wang H, Li J et al. Intracellular zinc release and ERK phosphorylation are required upstream of 12-lipoxygenase activation in peroxynitrite toxicity to mature rat oligodendrocytes. *J Biol Chem* 2006;281:9460-9470.
37. Szabó C, Day BJ, Salzman AL. Evaluation of the relative contribution of nitric oxide and peroxynitrite to the suppression of mitochondrial respiration in immunostimulated macrophages using a manganese mesoporphyrin superoxide dismutase mimetic and peroxynitrite scavenger. *FEBS Lett* 1996;381:82-86.
38. Fischer I. Candidate cells for transplantation into the injured CNS. *Prog Brain Res* 2000;128:253-257.
39. Lu KT, Wang YW, Yang JT et al. Effect of interleukin-1 on traumatic brain injury-induced damage to hippocampal neurons. *J Neurotrauma* 2005;22:885-895.
40. Cai Z, Pang Y, Lin S et al. Differential roles of tumor necrosis factor-alpha and interleukin-1 beta in lipopolysaccharide-induced brain injury in the neonatal rat. *Brain Res* 2003;975:37-47.
41. Shamash S, Reichert F, Rotshenker S. The cytokine network of Wallerian degeneration: tumor necrosis factor-alpha, interleukin-1alpha, and interleukin-1beta. *J Neurosci* 2002;22:3052-3060.
42. Hall ED, Springer JE. Neuroprotection and acute spinal cord injury: a reappraisal. *NeuroRx* 2004;1:80-100.
43. Li S, Stys PK. Mechanisms of ionotropic glutamate receptor-mediated excitotoxicity in isolated spinal cord white matter. *J Neurosci* 2000;20:1190-1198.
44. Liu NK, Zhang YP, Titsworth WL et al. A novel role of phospholipase A2 in mediating spinal cord secondary injury. *Ann Neurol* 2006;59:606-619.
45. Kawano T, Anrather J, Zhou P et al. Prostaglandin E2 EP1 receptors: downstream effectors of COX-2 neurotoxicity. *Nat Med* 2006;12:225-229.
46. Kwon KJ, Jung YS, Lee SH et al. Arachidonic acid induces neuronal death through lipoxygenase and cytochrome P450 rather than cyclooxygenase. *J Neurosci Res* 2005;81:73-84.

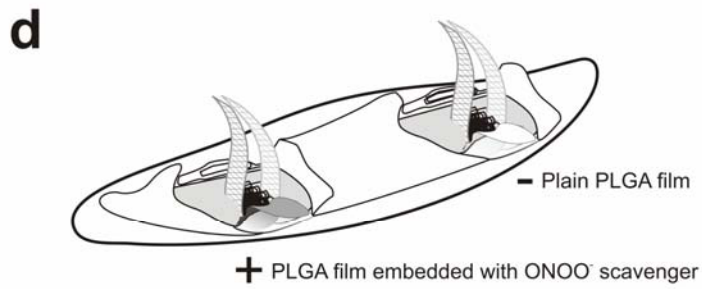
47. Manabe Y, Anrather J, Kawano T et al. Prostanoids, not reactive oxygen species, mediate COX-2-dependent neurotoxicity. *Ann Neurol* 2004;55:668–675.
48. Easton AS, Fraser PA. Arachidonic acid increases cerebral microvascular permeability by free radicals in single pial microvessels of the anaesthetized rat. *J Physiol* 1998;507:541–547.
49. Kulbatski I, Mothe AJ, Nomura H et al. Endogenous and exogenous CNS derived stem/progenitor cell approaches for neurotrauma. *Curr Drug Targets* 2005;6:111-126.
50. Iarikov DE, Kim BG, Dai HN et al. Delayed transplantation with exogenous neurotrophin administration enhances plasticity of corticofugal projections after spinal cord injury. *J Neurotrauma* 2007;24:690-702.
51. Yu D, Wilhelmsson U, Pekny M, Teng YD. A polymer scaffold mediated neural stem cell treatment for lower thoracic spinal cord injury in GFAP-/- Vimentin-/- mice. *Soc for Neurosci Abstract* 2008;online.
52. Beattie MS. Inflammation and apoptosis: linked therapeutic targets in spinal cord injury. *Trends Mol Med* 2004;10:580-583.
53. Conti A, Miscusi M, Cardali S et al. Nitric oxide in the injured spinal cord: synthases cross-talk, oxidative stress and inflammation. *Brain Res Rev* 2007;54:205-218.
54. Dalkara T, Yoshida T, Irikura K et al. Dual role of nitric oxide in focal cerebral ischemia. *Neuropharmacology* 1994;33:1447-1452.
55. Iadecola C. Bright and dark sides of nitric oxide in ischemic brain injury. *Trends Neurosci* 1997;20:132-139.
56. Madhavan L, Ourednik V, Ourednik J. Neural stem/progenitor cells initiate the formation of cellular networks that provide neuroprotection by growth factor-modulated antioxidant expression. *Stem Cells* 2008;26:254-265.
57. Peterson DA, Lucidi-Phillipi CA, Murphy DP et al. Fibroblast growth factor-2 protects entorhinal layer II glutamatergic neurons from axotomy-induced death. *J Neurosci* 1996;16:886-898.
58. Patel M, Day BJ. Metalloporphyrin class of therapeutic catalytic antioxidants. *Trends Pharmacol Sci* 1999;20:359-364.
59. Hunt JA, Lee J, Groves JT. Amphiphilic peroxy-nitrite decomposition catalysts in liposomal assemblies. *Chem Biol* 1997;4:845-858.
60. Bao F, DeWitt DS, Prough DS et al. Peroxy-nitrite generated in the rat spinal cord induces oxidation and nitration of proteins: reduction by Mn (III) tetrakis (4-benzoic acid) porphyrin. *J Neurosci Res* 2003;71:220-227.
61. Bao F, Liu D. Peroxy-nitrite generated in the rat spinal cord induces neuron death and neurological deficits. *Neuroscience* 2002;115:839-849.
62. Liu D, Bao F, Prough DS et al. Peroxy-nitrite generated at the level produced by spinal cord injury induces peroxidation of membrane phospholipids in normal rat cord: reduction by a metalloporphyrin. *J Neurotrauma* 2005;22:1123-1133.
63. Hachmeister JE, Valluru L, Bao F et al. Mn (III) tetrakis (4-benzoic acid) porphyrin administered into the intrathecal space reduces oxidative damage and neuron death after spinal cord injury: a comparison with methylprednisolone. *J Neurotrauma* 2006;23:1766-1778.
64. Bjugstad KB, Teng YD, Redmond DE Jr et al. Human neural stem cells migrate along the nigrostriatal pathway in a primate model of Parkinson's disease. *Exp Neurol* 2008;211:362-369.
65. Coyle JT, Puttfarcken P. Oxidative stress, glutamate, and neurodegenerative disorders. *Science* 1993;262:689-695.
66. Dumuis A, Sebben M, Haynes L et al. NMDA receptors activate the arachidonic acid cascade system in striatal neurons. *Nature* 1998;336:68-70.
67. Lazarewicz JW, Wroblewski JT, Palmer ME et al. Activation of N-methyl-D-aspartate-sensitive glutamate receptors stimulates arachidonic acid release in primary cultures of cerebellar granule cells. *Neuropharmacology* 1988;27:765-769.
68. Dawson TM, Dawson VL, Snyder SH. A novel neuronal messenger molecule in brain: the free radical, nitric oxide. *Ann Neurol* 1992;32:297-311.
69. Palmer LA, Gaston B, Johns RA. Normoxic stabilization of hypoxia-inducible factor-1 expression and activity: redox-dependent effect of nitrogen oxides. *Mol Pharmacol* 2000;58:1197-1203.
70. Hess DT, Matsumoto A, Kim SO, et al. Protein S-nitrosylation: purview and parameters. *Nat Rev Mol Cell Biol* 2005;6:150-166.
71. Feelisch M, Rassaf T, Mnaimneh S, et al. Concomitant S-, N-, and heme-nitros(yl)ation in biological tissues and fluids: implications for the fate of NO in vivo. *FASEB J* 2002;16:1775-1785.
72. Ricci-Vitiani L, Pedini F, Mollinari C, et al. Absence of caspase 8 and high expression of PED protect primitive neural cells from cell death. *J Exp Med* 2004;200:1257-1266.

See www.StemCells.com for supporting information available online.

Figure 1. Schematic of the *in vivo* study model. **a**, human neural stem cells (hNSCs) were seeded onto poly-lactic-*co*-glycolic (PLGA) scaffolds, and a porous nylon net was trimmed to deliver hNSC-coated scaffold in retrieval studies, but not in non-retrieval studies; **b**, PLGA films were embedded with a scavenger compound for ONOO⁻ (+), and control "plain" PLGA films were not embedded with drugs (-); **c**, dual penetrating spinal cord injury (SCI) model was created in rat spinal cord at T7-T8 and L2-L3 levels; **d**, the drug-embedded PLGA film is inserted at the bottom of the SCI cavity, followed by the placement of a nylon net-held scaffold seeded with hNSCs in retrieval studies or hNSC-seeded scaffolds only in non-retrieval studies (not shown); **e**, the extra length of the nylon net was folded for wound closure, and the drug-embedded PLGA film was folded to cover the lateral side of the implant; **f**, the scaffold was recovered by retrieving the nylon net at pre-determined time points for immunocytochemistry (ICC) analysis. Non-retrieval experiments were used for spinal cord tissue ICC analysis.



SCI model: dual penetrating injury model for same animal control



Co-implantation of PLGA film and retrievable scaffold seeded with hNSCs

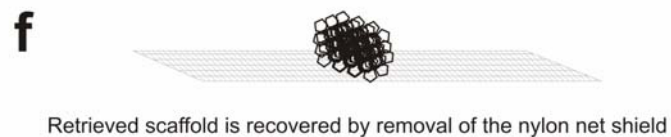
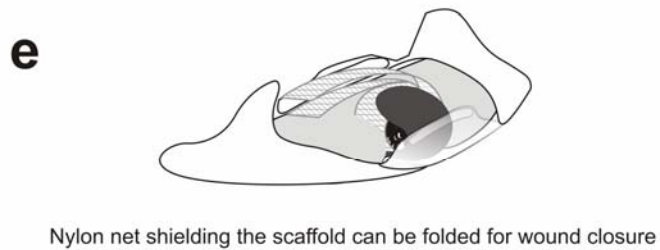


Figure 2. Annexin V-FLUOS assay. hNSCs were prepared as attached colonies on coverglass prior to drug stimulation: **a**, under the control condition, no drugs were given, and no cells displayed positive membrane stain profile of annexin V; **b**, stimulation using 400 μM 3-morpholinosydnonimine linsidomine chloride (SIN-1) for 3 h induced strong membrane staining profile for annexin V (green), but no propidium iodide staining (red) inside the cells; co-stimulation using SIN-1 (400 μM) with either, **c**, 100 μM (III) tetrakis (4-benzoic acid) porphyrin chloride (MnTBAP) or, **d**, 100 μM uric acid (UA) blocked the cell death effect of SIN-1; and **e**, stimulation with 20 μM glutamate induced neither positive propidium iodide staining, nor positive annexin V staining. For data presented in **f**, hNSCs prepared as suspension prior to drug stimulation demonstrated similar results to the attached cells, in that SIN-1 (200 and 400 μM) dose dependently induced positive annexin V staining pattern in significantly higher percentages of cells versus the negative outcome of the "plain" medium control or treatment with the NO donor (Z)-1-{N-[3-Aminopropyl]-N-[4-(3-aminopropylammonio)butyl]-amino}-diazene-1-ium-1,2-diolate (spermine NONOate, 200 μM ; error bars represent standard error, n = 3, * $p < 0.05$, paired t -test, details see Supplementary Table). Importantly, 200 μM MnTBAP or UA treatment markedly mitigated such cell death triggered by exposure to SIN-1. Scale bar = 500 μm .

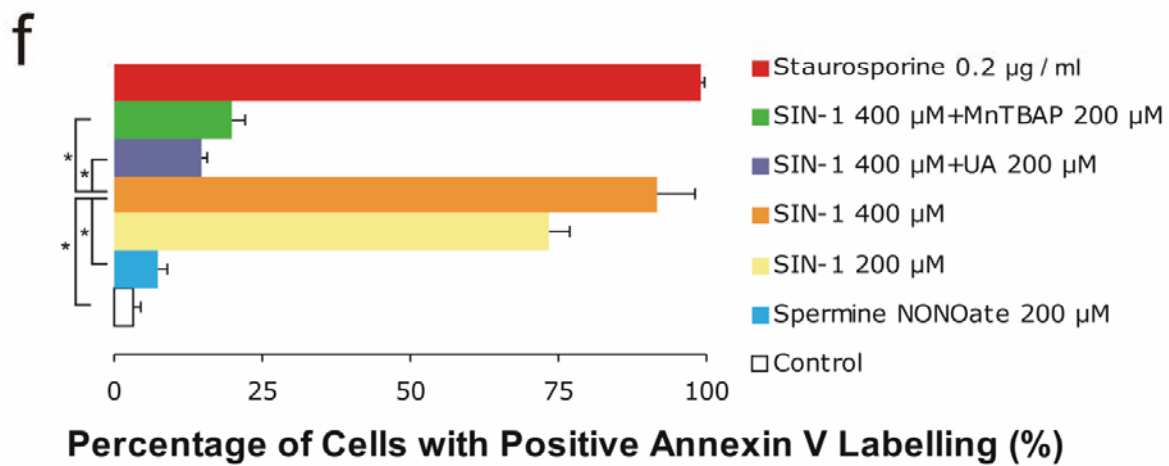
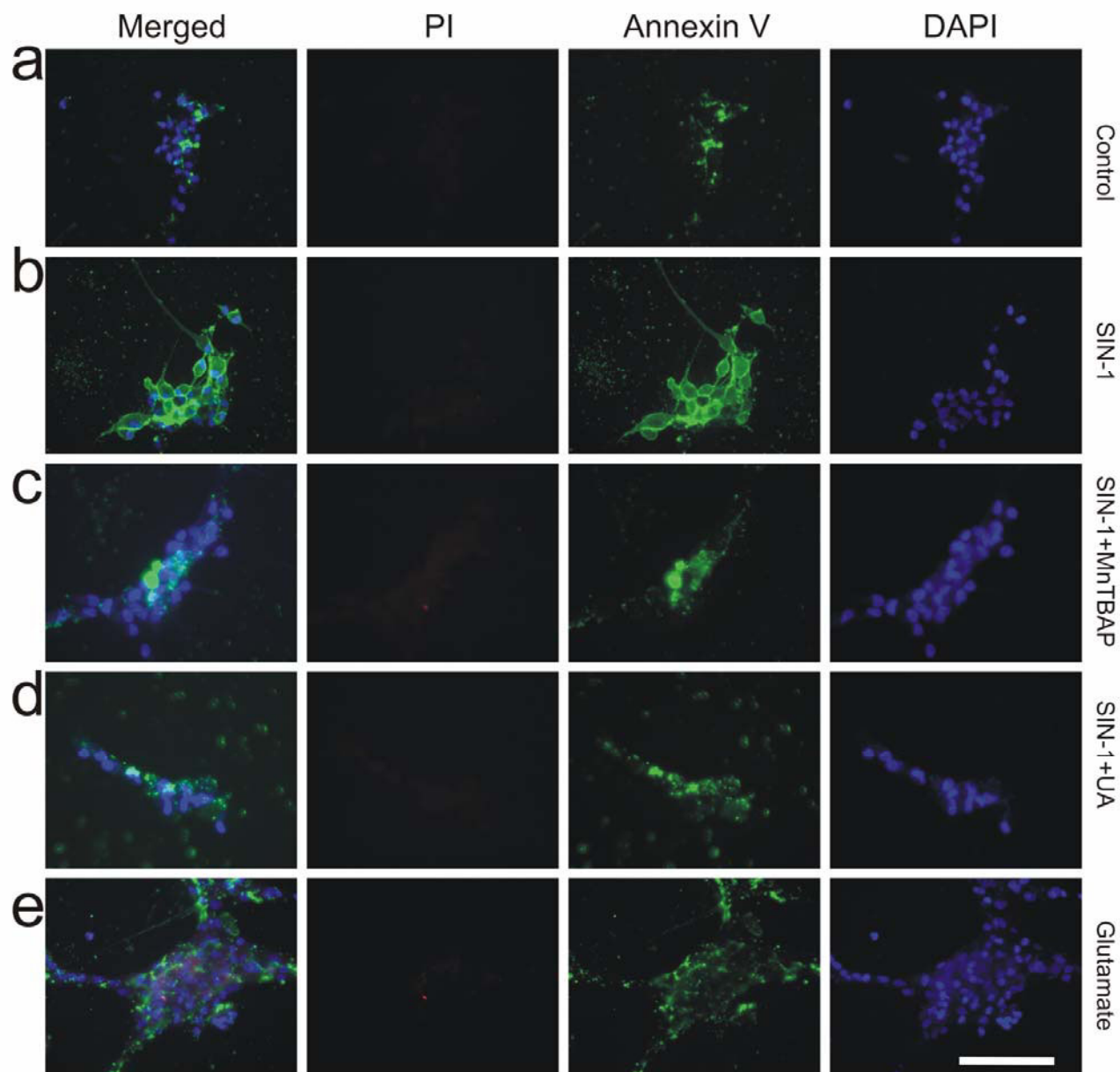


Figure 3. TUNEL assay. Human NSCs were prepared as attached colonies on coverglass prior to drug stimulation: **a**, under the control condition, no cells displayed positive nuclear stain profile of TUNEL labeling (green); **b**, stimulation using 400 μ M SIN-1 for 3 h induced strong nuclear staining profile (green), overlapping with DAPI stain (blue); co-stimulation using SIN-1 (400 μ M) with either 100 μ M MnTBAP (**c**) or 100 μ M UA (**d**) blocked the SIN-1 effect. Additionally, hNSCs prepared as suspension prior to drug stimulation demonstrated similar results to the attached cells (**e**), in that SIN-1 (200 and 400 μ M) induced positive TUNEL staining pattern in significantly higher percentages of cells than "plain" medium control or treatment with spermine NONOate (200 μ M; error bars represent SEM, $n = 3$, $*p < 0.05$, paired t -test, details see Supplementary Table). Both MnTBAP and UA (200 μ M) diminished the cell death effect of SIN-1. Scale bar = 500 μ m.

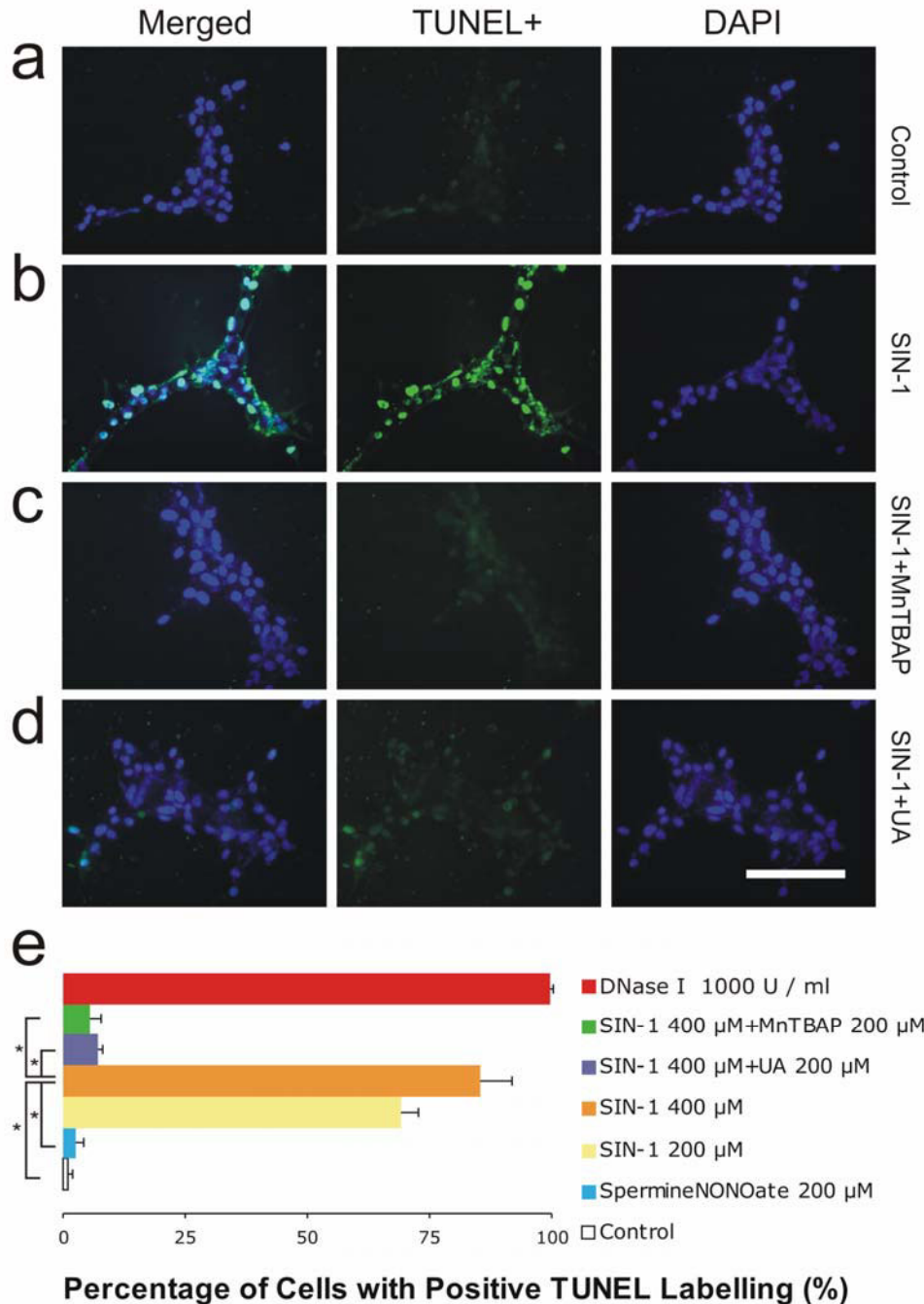


Figure 4. Nitrotyrosine immunocytochemistry (ICC). All hNSCs were ICC positive for the human marker, heat-shock protein 27 (hHsp; green). **a**, under the control condition, no drugs were added to the culture medium, and no nitrotyrosine was detected (red); **b**, stimulation using SIN-1 (400 μ M) induced high levels of detectable protein nitration, showing positive nitrotyrosine staining (red) in nearly every cell. Co-administration of either 100 μ M MnTBAP (**c**) or 100 μ M UA (**d**) eliminated this effect. Scale bar = 500 μ m.

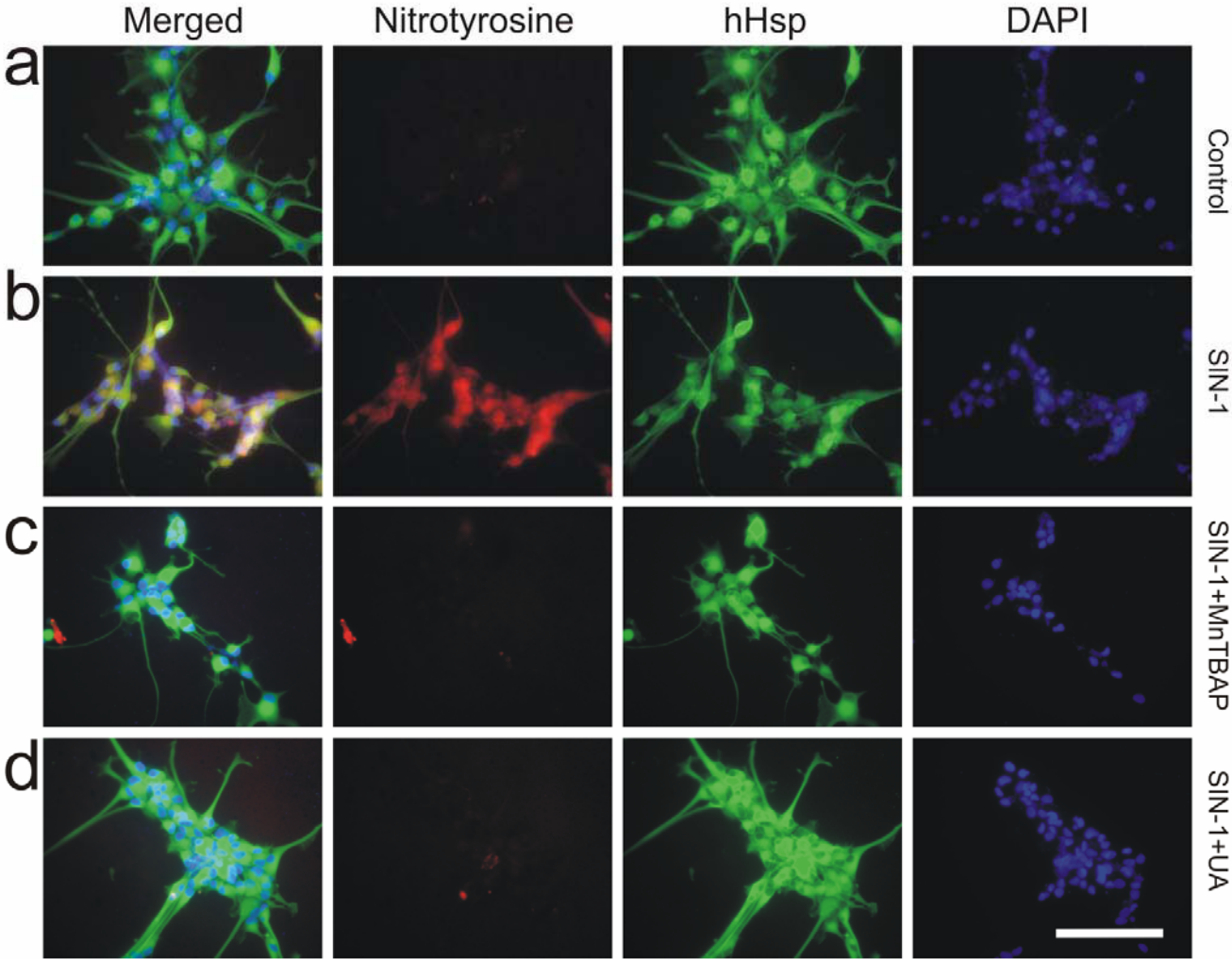


Figure 5. The cell death signaling pathways that were activated by SIN-1 exposure. **a**, Western Blot assay indicated that SIN-1 (400 μM) treatment strongly stimulated Erk phosphorylation in hNSCs, relative to the control (no drug) or spermine NONOate (400 μM) exposure. Either MnTBAP or UA (200 μM) mitigated this effect of SIN-1; **b**, a similar stimulating effect was observed in p38 phosphorylation; **c**, ICC co-localizations (arrows) of phospho-p38 (red) and human mitochondria (hMito; green; scale bar = 50 μm) were present in SIN-1 (400 μM) stimulated cells only; **d**, cytochrome *c* (Cy *c*) release from mitochondria to the cytosol is a trigger for the activation of downstream caspases. SIN-1 (100 and 400 μM) dose dependently stimulated this process, while the NO donor (DETA NONOate, or DETA: 100 or 400 μM) had very little effect. Staurosporine (0.2 $\mu\text{g/ml}$) was used as positive control, and control proteins (CP: COX4 for mitochondria, β -actin for cytosol) were used to ensure equal loading of protein for each assay; **e**, ICC detection of mitochondrial release of cytochrome *c* (green; scale bar = 50 μm) to the cytosol was only seen in SIN-1 (400 μM) stimulated cells; **f**, Western Blot for caspase 3 showed that only SIN-1 (100 and 400 μM) stimulated caspase 3 activation; **g**, the cleaved (activated) form of caspase 3 (green; scale bar = 500 μm) was only observed in hNSCs (red; human nestin or hNestin) exposed to SIN-1 (400 μM); **h**, Caspase assays: the whole cell lysate of hNSCs treated with different drugs was used. Both caspase 3 and caspase 9 showed significant activation following SIN-1 (200 and 400 μM) stimulation relative to the control (i.e., plain medium) or exposure to spermine NONOate (200 μM , NO donor; error bars represent SEM, $n = 3$, $*p < 0.05$, paired *t*-test, details see Supplementary Table). Co-administration of MnTBAP (200 μM) significantly reduced activation of both caspases, and there was no significant detections/changes in caspase 8 in the SIN-1 (400 μM) treated samples (data not shown) due to its known absence in NSCs [72].

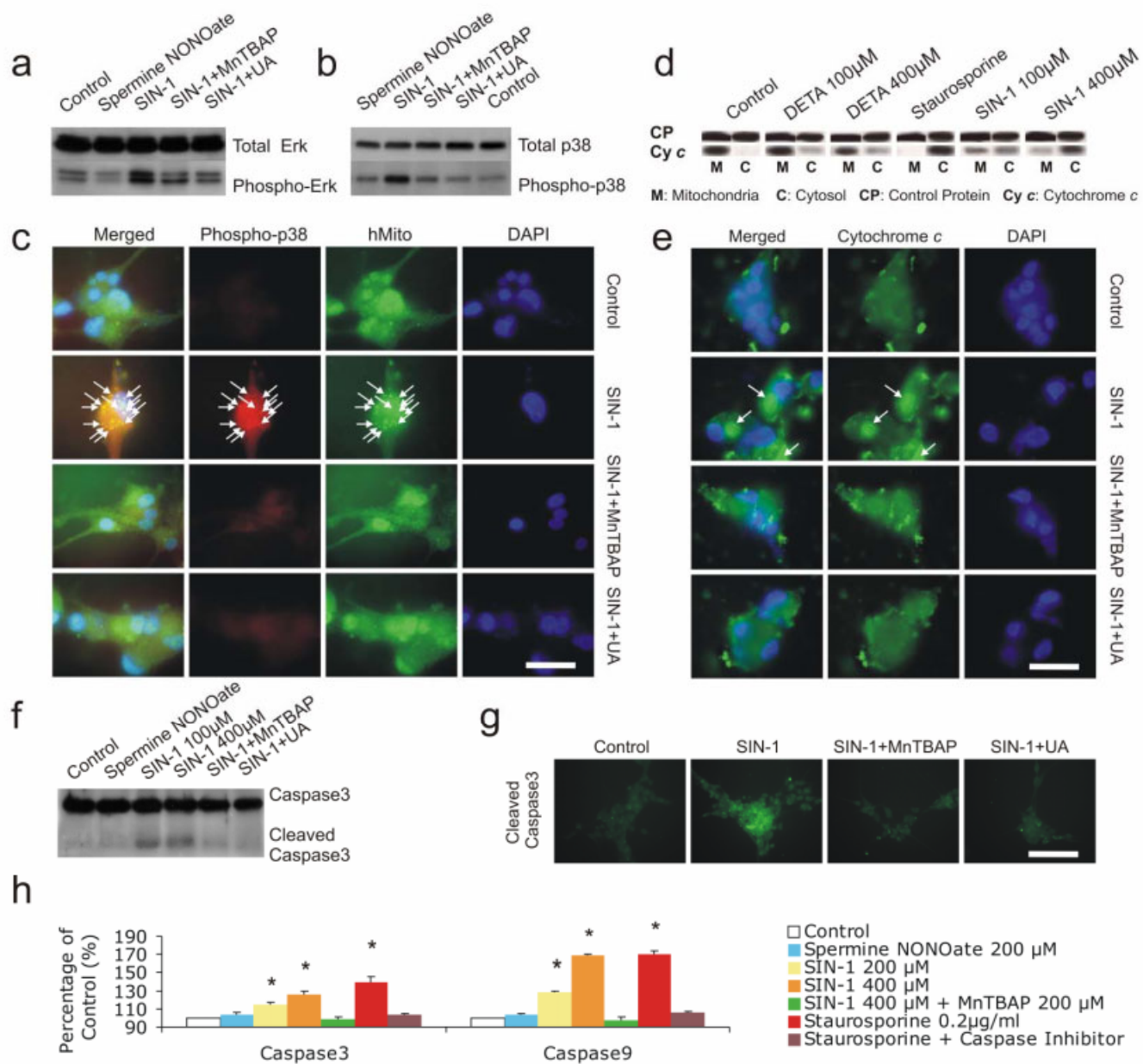
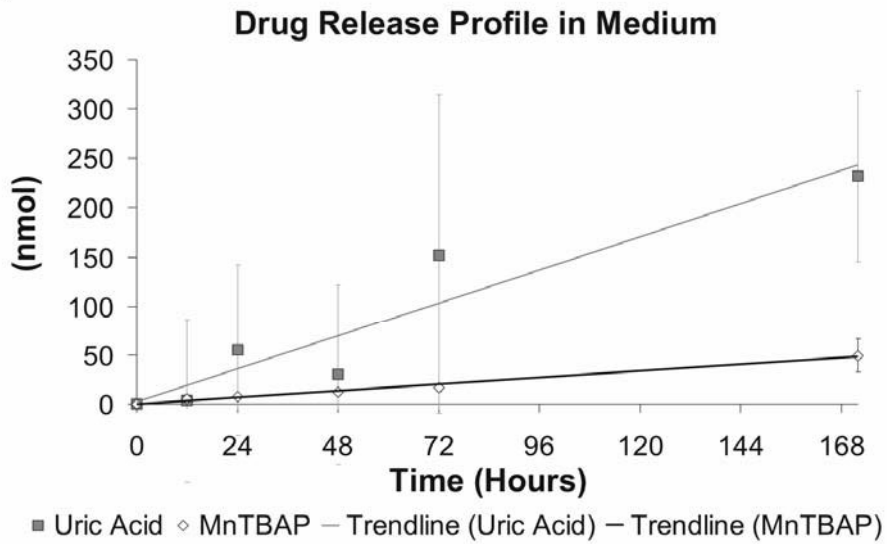
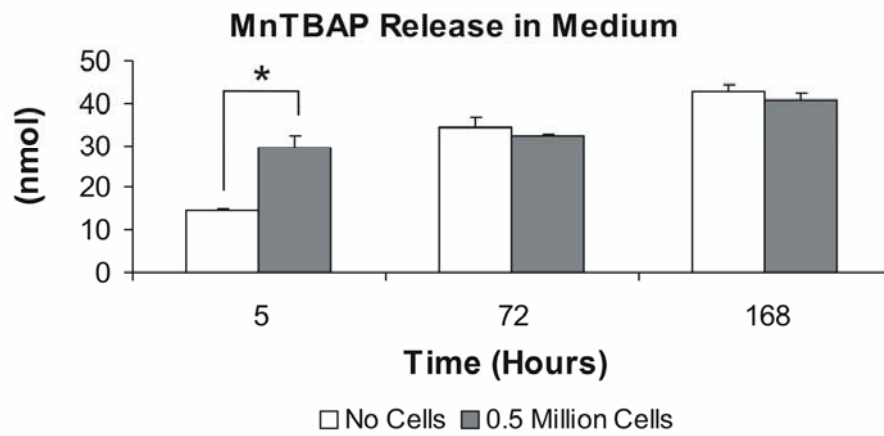


Figure 6. Polymer drug release profiles. **a**, quantitative measurement of UA and MnTBAP showed that both compounds had sustainable release from PLGA films in cell culture medium over a time course of 172 h (error bars represent 95% confidence interval; there was no significant difference between the two groups; $p > 0.26$, two-way repeated measures ANOVA); **b**, the presence of hNSCs (0.5 million/5 ml) in the medium significantly increased the rate of release within 5 h of incubation (error bars represent SEM, $n = 3$, $*p = 0.0134$). However, hNSC presence did not change the longer term release amount of the embedded drugs; **c**, the selective fluorescent indicator for ONOO⁻, dihydrorhodamine 123 (DHR123), showed that MnTBAP released from PLGA films significantly reduced SIN-1 (400 μ M)-derived ONOO⁻ levels in the medium (error bars represent SEM, $n = 3$, $*p < 0.0005$, paired t -test, details see Supplementary Table).

a



b



c

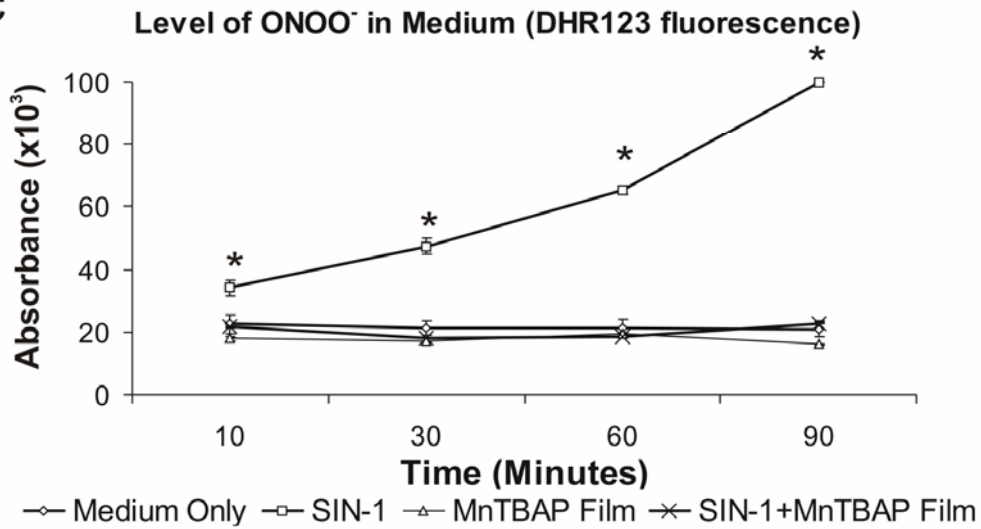


Figure 7. Drug-releasing polymer films protected hNSCs *in vivo*. The sign (-) indicates co-transplantation of hNSC-seeded scaffolds with drug-free "plain" PLGA films, and (+), with films containing MnTBAP, an ONOO⁻ scavenger, into the injury epicenter of the spinal cord. Examination of hNSCs recovered at 24 h post SCI demonstrated the following findings. **a**, ICC co-localizing of phospho-p38 (green) and the donor cell marker hNestin (red), revealed that shielding with MnTBAP-releasing PLGA film markedly impeded activation of cell death signaling in donor hNSCs (+, bottom row, arrows), compared to the controls (-, top row); **b**, co-staining of nitrotyrosine (red) and the donor cell marker hHsp (green) showed high levels of ONOO⁻ impact on most hNSCs when not treated with MnTBAP (-, top row, arrows), and co-implantation of MnTBAP-releasing PLGA films mitigated ONOO⁻ exposure to hNSCs (+, bottom row); **c**, ICC co-localization of active/cleaved caspase 3 (green) and the donor cell marker hHsp (red) showed high frequency of hNSC apoptosis under no MnTBAP treatment (-, top row, arrows). In contrast, MnTBAP released from PLGA films impeded caspase 3 activation in hNSCs (+, bottom row); **d**, relative to the controls (-), implantation of MnTBAP-releasing PLGA films effectively inhibited caspase 3 activation and ONOO⁻ reactivity (nitrotyrosine) in the host tissue adjacent to the injury epicenter. Scale bars: a, b = 200 μm; c = 250 μm; d = 500 μm. Dotted line-delineated area: autofluorescent polymer scaffolds.

